

## SIMULATION OF FREE-RISING BUBBLE WITH SOLUBLE SURFACTANT USING MOVING MESH FINITE VOLUME/AREA METHOD

Zeljko Tukovic<sup>\*,1</sup> and Hrvoje Jasak<sup>1,2</sup>

<sup>1</sup>Faculty of Mechanical Engineering and Naval Architecture, Zagreb, Croatia

<sup>2</sup>Wikki Ltd., London, England

\* E-mail: Zeljko.Tukovic@fsb.hr

### ABSTRACT

In this study, flow simulation of the two-fluid system with sharp interface and soluble surfactants is performed using OpenFOAM, an object-oriented C++ library for simulations in continuum mechanics. The Finite Volume method with moving computational mesh support is used to implement an interface-tracking procedure, where each fluid phase is associated with a separate mesh which moves and deforms according to interface motion. Mathematical model governing incompressible fluid flow is solved on each moving mesh separately and coupling is accomplished by enforcing the kinematic and dynamic conditions at the interface. Surfactant adsorption/desorption at the interface is modelled using the Langmuir kinetic law, while surface tension is calculated from surfactant concentration at the interface using the nonlinear Frumkin-Langmuir equation of state. Surfactant transport along the interface is calculated using a Finite Area Method for discretisation of surface transport equation on a curved and moving unstructured surface mesh. The numerical procedure is used to simulate the effects of soluble surfactants on the motion of a free-rising air bubble in still water. The bubble of 2 mm diameter is considered, where experiments show ellipsoidal bubble shape and motion along a zig-zag and/or a helicoidal path. Calculations are performed for a clean and contaminated bubble and the results shows good agreement with available experimental data.

**Keywords:** finite volume method, finite area method, moving mesh, interface tracking, soluble surfactants, free-rising bubble.

### INTRODUCTION

Behaviour of multi-phase systems with sharp interfaces is significantly influenced by the presence of chemicals that accumulate on the phase interface and influence its properties. Surfactants (surface active agents) are substances whose molecules possess a bipolar structure, *i.e.*

polar (hydrophilic) head and apolar (hydrophobic) tail, what cause their adsorption on the interface between the polar (aqueous) and apolar (non-aqueous) fluid phases. They are convected and diffused both at the interface and in the bulk fluid and their presence at the interface alters the interfacial tension, resulting in a highly non-linear interaction between fluid flow and surfactant concentration. Therefore, governing equations of surfactant transport at the interface and in the bulk must be closely coupled with the flow equations.

Previous computational studies of the effect of surfactants using full Navier-Stokes model can be classified according to the applied numerical methodology: volume-of-fluid method [Drumright-Clarke and Renardy (2004), James and Lowengrub (2004)], Peskin's immersed-interface method [Lee and Pozrikidis (2006)] level-set method [Xu et al. (2006)], and front-tracking method [Zhang et al. (2006), Muradoglu and Tryggvason (2008)].

This paper presents numerical methodology for simulation of two-fluid system with a sharp interface and soluble surfactant using interface tracking method based on finite volume discretisation, moving computational mesh and automatic mesh motion. Although such approach is limited to moderate interface deformation with the constant interface topology, it potentially offers highest accuracy because interface is represented by the computational mesh boundary. Cases with large interface deformation can also be simulated using this approach by applying local topological change in the mesh, including surface break-up.

In the next section, the governing equations for two-fluid system with the sharp interface and soluble surfactants are described. After description of discretisation for volumetric and surface equations on moving computational mesh using finite volume/area method, interface tracking solution procedure is described. Finally, the performance of the method is presented in a simulation of motion of free-rising air bubble in clean and contaminated water.

## MATHEMATICAL MODEL

In this study a two-phase fluid flow with sharp interface is simulated using the Finite Volume method and a moving computational mesh. On each phase, one defines a separate computational mesh which moves and deforms according to interface motion. Mathematical model governing the isothermal flow of incompressible fluid is solved on each moving mesh separately and coupling is accomplished by the enforcement of proper boundary conditions at the interface.

Isothermal flow of incompressible Newtonian fluid inside an arbitrary volume  $V$  bounded by a closed surface  $S$  is governed by the mass and linear momentum conservation laws:

$$\oint_S \mathbf{n} \cdot \mathbf{v} \, dS = 0, \quad (1)$$

$$\begin{aligned} \frac{d}{dt} \int_V \rho \mathbf{v} \, dV + \oint_S \mathbf{n} \cdot \rho (\mathbf{v} - \mathbf{v}_s) \mathbf{v} \, dS \\ = \oint_S \mathbf{n} \cdot (\mu \nabla \mathbf{v}) \, dS - \int_V \nabla p \, dV. \end{aligned} \quad (2)$$

where  $\mathbf{n}$  is outward pointing unit normal vector on  $S$ ,  $\rho$  is the fluid density,  $\mathbf{v}$  is the fluid velocity,  $\mathbf{v}_s$  is the velocity of  $S$ ,  $\mu$  is the dynamic viscosity of a fluid and  $p$  is the dynamic pressure obtained by subtracting hydrostatic pressure,  $\rho \mathbf{g} \cdot \mathbf{r}$ , from the absolute pressure, where  $\mathbf{g}$  is the gravitational acceleration and  $\mathbf{r}$  is the position vector. The relationship between the rate of change of the volume  $V$  and the velocity  $\mathbf{v}_s$  is defined by the *space conservation law* [Demirdžić and Perić (1988)]:

$$\frac{d}{dt} \int_V dV - \oint_S \mathbf{n} \cdot \mathbf{v}_s \, dS = 0. \quad (3)$$

The formulation of the above mathematical model is known as arbitrary Lagrangian-Eulerian formulation (ALE).

If the fluid phases are immiscible, fluid flow equations (1) and (2) can be applied for each phase separately, while on the interface the proper boundary conditions must be used. Relation between fluid velocities on the two sides of the interface is determined by the *kinematic condition* (Batchelor (1967)), according to which the velocity must be continuous across the interface:

$$\mathbf{v}_1 = \mathbf{v}_2. \quad (4)$$

Here,  $\mathbf{v}_1$  and  $\mathbf{v}_2$  are fluid velocities at the two sides of the interface.

From the momentum conservation law follows the *dynamic condition*, which states that forces acting on the fluid at the interface are in equilibrium. From the normal force balance follows the *pressure jump conditions*:

$$p_2 - p_1 = \sigma \kappa - 2(\mu_2 - \mu_1) \nabla_s \cdot \mathbf{v}, \quad (5)$$

where  $\sigma$  is the surface tension coefficient,  $\kappa = -\nabla_s \cdot \mathbf{n}$  is twice the mean curvature of the interface,  $\nabla_s = \nabla - \mathbf{nn} \cdot \nabla$  is the surface gradient operator and  $\mathbf{n}$  is a unit normal vector at the interface which points from fluid 1 to fluid

2. Relation between normal derivative of velocity at the two sides of the interface follows from the tangential force balance and reads:

$$\begin{aligned} \mu_2 [\mathbf{n} \cdot (\nabla \mathbf{v})_2] - \mu_1 [\mathbf{n} \cdot (\nabla \mathbf{v})_1] = \\ - \nabla_s \sigma - \mathbf{n} (\mu_2 - \mu_1) \nabla_s \cdot \mathbf{v} - (\mu_2 - \mu_1) (\nabla_s \mathbf{v}) \cdot \mathbf{n}. \end{aligned} \quad (6)$$

The surface tension gradient  $\nabla_s \sigma$  will occur due to nonuniform distribution of surfactants at the interface. In this study, the surface tension is related to the surfactant concentration on the interface by the nonlinear Frumkin-Langmuir equation of state [Edwards et al. (1991)]:

$$\sigma = \sigma_0 + \mathcal{R}T\Phi_\infty \ln \left( 1 - \frac{\Phi}{\Phi_\infty} \right), \quad (7)$$

where  $\sigma_0$  is the surface tension of a clean interface,  $\Phi$  is the surfactant concentration at the interface,  $\Phi_\infty$  is the saturated surfactant concentration,  $\mathcal{R}$  is the universal gas constant and  $T$  is the temperature.

The transport of surfactant in the bulk fluid of arbitrary volume  $V$  is governed by the following integral transport equation:

$$\begin{aligned} \frac{d}{dt} \int_V C \, dV + \oint_S \mathbf{n} \cdot (\mathbf{v} - \mathbf{v}_s) C \, dS \\ = \oint_S \mathbf{n} \cdot (D \nabla C) \, dS, \end{aligned} \quad (8)$$

where  $C$  is the bulk surfactant concentration and  $D$  is the bulk surfactant diffusion coefficient.

Governing equation for surfactant transport along an arbitrary surface  $S$  on the interface, bounded by a closed curve  $\partial S$  reads:

$$\begin{aligned} \frac{d}{dt} \int_S \Phi \, dS + \oint_{\partial S} \mathbf{m} \cdot (\mathbf{v}_t - \mathbf{b}_t) \Phi \, dL \\ = \oint_{\partial S} \mathbf{m} \cdot (D_s \nabla_s \Phi) \, dL + \int_S s_\Phi \, dS, \end{aligned} \quad (9)$$

where  $\mathbf{m}$  is the outward pointing unit bi-normal on  $\partial S$ ,  $\mathbf{v}_t = (\mathbf{I} - \mathbf{nn}) \cdot \mathbf{v}$  is the tangential component of fluid velocity at the interface,  $\mathbf{b}_t$  is the velocity at which curve  $\partial S$  moves along the interface,  $L$  is the arc length measured along  $\partial S$ ,  $D_s$  is the diffusion coefficient of the surfactant along the interface and  $s_\Phi$  is the source/sink of surfactant per unit area due to adsorption and desorption.

Transport of surfactant between bulk fluid and interface due to adsorption and desorption process is described by the Langmuir's kinetics laws [Edwards et al. (1991)]:

$$s_\Phi = k_a [C_s (\Phi_\infty - \Phi) - \beta \Phi], \quad (10)$$

where  $k_a$  and  $\beta$  are the parameters of the adsorption and desorption kinetics, respectively, and  $C_s$  is the limiting value of  $C$  at the interface. Normal derivative of bulk surfactant concentration at the interface is calculated using following expression:

$$[\mathbf{n} \cdot \nabla C]_{interface} = -\frac{s_\Phi}{D}. \quad (11)$$

## FINITE VOLUME/AREA DISCRETISATION AND SOLUTION PROCEDURE

In this study, the cell-centred finite volume method (FVM) is used for discretisation of bulk fluid models and the face-centred finite area method (FAM) is used for discretisation of surfactant transport model along the interface. The finite volume/area discretisation is based on the integral form of the conservation equation over a fixed or moving control volume/area. The discretisation procedure is divided into two parts: discretisation of the computational domain and equation discretisation.

### Discretisation of the computational domain

The discretisation of the computational domain consists of the discretisation of the time interval and the discretisation of space. The time interval is split into a finite number of time-steps  $\Delta t$  and the equations are solved in a time-marching manner. Unstructured FVM discretises the computational space by splitting it into a finite number of convex polyhedral control volumes (CV) or cells bounded by convex polygons. The cells do not overlap and fill the spatial domain completely. Figure 1 shows a sample polyhedral control volume  $V_P$  around the computational point  $P$  located in its centroid, the face  $f$ , the face area  $S_f$ , the face unit normal vector  $\mathbf{n}_f$  and the centroid  $N$  of the neighbouring CV sharing the face  $f$ . The geometry of the CV is fully determined by the position of its vertices.

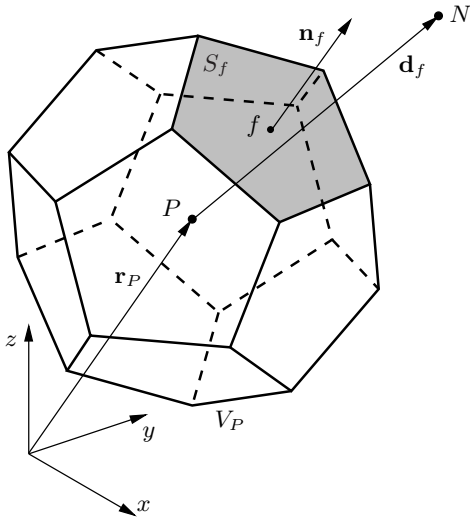


Figure 1: Polyhedral control volume (cell).

The finite volume mesh must be adjusted to the time varying shape of the interface. The deforming mesh approach is used in this study where the internal CV vertices are moved based on the prescribed motion of the boundary vertices while the topology of the mesh stays unchanged. The vertex-based automatic mesh motion solver developed by the authors [Jasak and Tuković (2006); Tuković (2005)] is used for mesh deformation. Here, the Laplace mesh motion equation is discretised on the composite polyhedral element using the Finite Element Method (FEM). In order to control mesh quality,

the variable diffusion inversely proportional to the distance from the moving boundary is used with the Laplace mesh motion equation.

The polygonal cell faces which coincide with the interface constitute the Finite Area mesh on which the surfactant transport equation is discretised. Figure 2 shows a sample polygonal control area  $S_P$  around the computational point  $P$  located in its centroid, the edge  $e$ , the edge length  $L_e$ , the edge unit bi-normal vector  $\mathbf{m}_e$  and the centroid  $N$  of the neighbouring control area sharing the edge  $e$ . The bi-normal  $\mathbf{m}_e$  is perpendicular to the edge normal  $\mathbf{n}_e$  and to the edge vector  $\mathbf{e}$ .

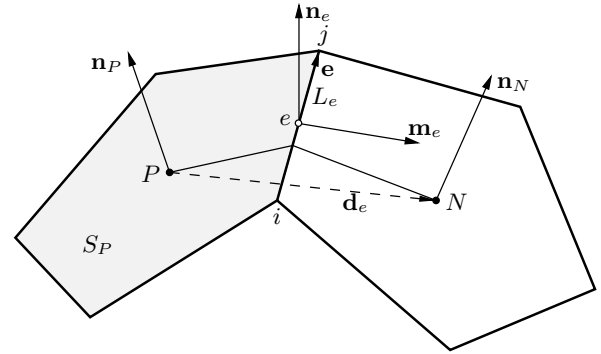


Figure 2: Polygonal control area.

### Discretisation of volumetric equations

The second-order FV discretisation of an integral conservation equation transforms the surface integrals into sums of face integrals and approximates them and the volume integrals to the second order accuracy by using the mid-point rule. The spatially discretised form of momentum equation (2) for the moving control volume  $V_P$  reads:

$$\begin{aligned} \frac{d(\rho_P \mathbf{v}_P V_P)}{dt} + \sum_f (\dot{m}_f - \rho_f \dot{V}_f) \mathbf{v}_f \\ = \sum_f \mu_f \mathbf{n}_f \cdot (\nabla \mathbf{v})_f S_f + (\nabla p)_P V_P, \end{aligned} \quad (12)$$

where the subscripts  $P$  and  $f$  represent the cell-centre and face-centre values. The face mass flux  $\dot{m}_f = \rho_f \mathbf{n}_f \cdot \mathbf{v}_f S_f$  must satisfy the discretised mass conservation law while the face volume flux  $\dot{V}_f$  must satisfy the discretised SCL, Eq. (3). Evaluation of volume fluxes will be explained later in this section.

The face-centre values of all dependent variables are calculated using linear interpolation of the neighbouring cell-centre values. The exception is the face value of the dependent variable in the convection term [ $\mathbf{v}_f$  in Eq. (12)] which is calculated using the Gamma interpolation scheme [Jasak et al. (1999)] which locally blends second order accurate linear interpolation with the unconditionally bounded upwind interpolation to ensure boundedness.

The face normal derivative  $\mathbf{n}_f \cdot (\nabla \mathbf{v})_f$  in the diffusion term is discretised as follows [see Jasak (1996)]:

$$\mathbf{n}_f \cdot (\nabla \mathbf{v})_f = \underbrace{|\Delta_f| \frac{\mathbf{v}_N - \mathbf{v}_P}{|\mathbf{d}_{fu}|}}_{\text{Orthogonal contribution}} + \underbrace{(\mathbf{n}_f - \Delta_f) \cdot (\nabla \mathbf{v})_f}_{\text{Non-orthogonal correction}}, \quad (13)$$

where  $\Delta_f = \frac{\mathbf{d}_f}{\mathbf{d}_f \cdot \mathbf{n}_f}$ , Fig. 1. The orthogonal contribution in Eq. (13) is treated implicitly, while the non-orthogonal correction is explicit.

The face mass flux in the non-linear convection term and the non-linear surface source term are treated explicitly after the discretisation, *i.e.* their values from previous iteration are used.

The cell-centre gradient of dependent variables used for the calculation of the explicit source terms and the non-orthogonal correction in Eq. (13), is obtained by using the least-squares fit [Demirdžić and Muzaferija (1995)], [Jasak and Weller (2000)]. This method produces a second-order accurate gradient irrespective of the mesh quality.

The **temporal discretisation** of all equations is performed by using the second-order accurate implicit three time level scheme [Ferziger and Perić (1995)] referred to as the backward scheme. All terms of Eq. (12) are evaluated at the new time instance  $t^n = t^o + \Delta t$  and the temporal derivative is discretised by using two old-time levels:

$$\left( \frac{\partial \mathbf{v}}{\partial t} \right)^n = \frac{3\mathbf{v}^n - 4\mathbf{v}^o + \mathbf{v}^{oo}}{2\delta t}, \quad (14)$$

where  $\mathbf{v}^n = \mathbf{v}(t^o + \delta t)$ ,  $\mathbf{v}^o = \mathbf{v}(t^o)$  and  $\mathbf{v}^{oo} = \mathbf{v}(t^o - \delta t)$ .

When Eq. (13) and Eq. (14) are substituted into Eq. (12) and convection discretisation scheme is applied, the discretised form of the momentum equation (2) can be written in the form of linear algebraic equation, which for cell  $P$  reads:

$$a_P \mathbf{v}_P^n + \sum_N a_N \mathbf{v}_N^n = \mathbf{r}_P + (\nabla p)_P V_P, \quad (15)$$

where the diagonal coefficient  $a_P$ , the neighbour coefficient  $a_N$  and the source term  $\mathbf{r}_P$  can be found in Tuković (2005).

The mathematical model of fluid flow is solved using segregated solution procedure where momentum equation is solved decoupled from the pressure equation. **Discretised pressure equation**, obtained by combining discretised momentum and continuity equations, reads [Jasak (1996)]:

$$\sum_f \left( \frac{V_P^n}{a_P} \right)_f \mathbf{n}_f \cdot (\nabla p)_f^n S_f^n = \sum_f \mathbf{n}_f \cdot \left( \frac{\mathbf{H}_P(\mathbf{v}^n)}{a_P} \right)_f S_f^n \quad (16)$$

where

$$\mathbf{H}_P(\mathbf{v}^n) = - \sum_f a_N \mathbf{v}_N^n + r_P, \quad (17)$$

and face normal derivative of pressure at the left hand side of Eqn. (16) is discretised using expression (13). The absolute mass flux  $\dot{m}_f^n$  through the cell face  $f$  is calculated as follows:

$$\dot{m}_f^n = \rho_f \mathbf{n}_f \cdot \left[ \left( \frac{\mathbf{H}_P(\mathbf{v}^n)}{a_P} \right)_f - \left( \frac{V_P^n}{a_P} \right)_f (\nabla p)_f^n \right] S_f^n. \quad (18)$$

Mass flux calculated in this manner will satisfy the discretised continuity equation if the pressure field satisfies the pressure equation (16).

Demirdžić and Perić (1988) showed that failure to satisfy the **space conservation law** (SCL) on moving meshes introduces errors in the form of artificial mass sources. It is also showed that temporal discretisation scheme used for SCL should be the same as that for other considered conservation equations.

Discretised counterpart of the SCL where backward scheme is used for temporal discretisation reads:

$$\frac{3V_P^n - 4V_P^o + V_P^{oo}}{2\Delta t} - \sum_f \dot{V}_f^n = 0. \quad (19)$$

The difference between the cell volumes at consecutive time-levels can be decomposed as follows:

$$V_P^n - V_P^o = \sum_f \delta V_f^n, \quad (20)$$

where  $\delta V_f^n$  is the volume swept by the cell face  $f$  while moving from its old position to its new position. Substitution of Eq. (20) into Eq. (19) yields:

$$\frac{1}{2\Delta t} \sum_f (3\delta V_f^n - \delta V_f^o) = \sum_f \dot{V}_f^n. \quad (21)$$

Hence, if the backward temporal discretisation scheme is used, the cell faces volume fluxes are calculated using the following expression:

$$\dot{V}_f^n = \frac{3}{2} \frac{\delta V_f^n}{\Delta t} - \frac{1}{2} \frac{\delta V_f^o}{\Delta t}, \quad (22)$$

and the discretised SCL is satisfied identically.

## Discretisation of surface equations

Applying second-order collocated finite area method, **surfactant transport equation** (9) can be discretised on the moving control area  $S_P$  (see Fig. 2) as follows:

$$\frac{d(\Phi_P S_P)}{dt} + \sum_e \mathbf{m}_e \cdot (\mathbf{v}_t)_e L_e \Phi_e = \sum_e D_e \mathbf{m}_e \cdot (\nabla \Phi)_e L_e + (s_\Phi)_P S_P, \quad (23)$$

where the subscripts  $P$  and  $e$  represent the face-centre and edge-centre values, and  $(\mathbf{b}_t)_e = 0$ .

The edge-centre tangential velocity  $\mathbf{v}_t$  is calculated using following linear interpolation formula:

$$(\mathbf{v}_t)_e = (\mathbf{T}_e)^T \cdot [e_x \mathbf{T}_P \cdot (\mathbf{v}_t)_P + (1 - e_x) \mathbf{T}_N \cdot (\mathbf{v}_t)_N]. \quad (24)$$

where  $e_x$  is the interpolation factor which is calculated as the ratio of the geodetic distances  $\overline{eN}$  and  $\overline{PeN}$  (Fig. 2):

$$e_x = \frac{\overline{eN}}{\overline{PN}}, \quad (25)$$





as starting point for a derivation of novel procedure for calculation of surface tension forces.

Let us assume the interface is discretised with unstructured surface mesh consisting of arbitrary polygonal control areas. Surface tension force acting on the control area  $S_{Af}$  (see Fig. 7) can be expressed by the following equation:

$$\mathbf{F}_{1f}^\sigma = \oint_{\partial S_{Af}} \mathbf{m}\sigma \, dL = \sum_e \int_{L_e} \mathbf{m}\sigma \, dL = \sum_e \sigma_e \mathbf{m}_e L_e, \quad (41)$$

where  $\sigma_e$  and  $\mathbf{m}_e$  are the surface tension and bi-normal unit vector at the centre of the edge  $e$  and  $L_e$  is the length of the edge  $e$ . If the total surface tension force for each control area in the mesh is calculated using Eq. (41), then the total surface tension force for a closed surface will be exactly zero if unit bi-normals  $\mathbf{m}_e$  for two control areas sharing the edge  $e$  are parallel and have opposite direction.

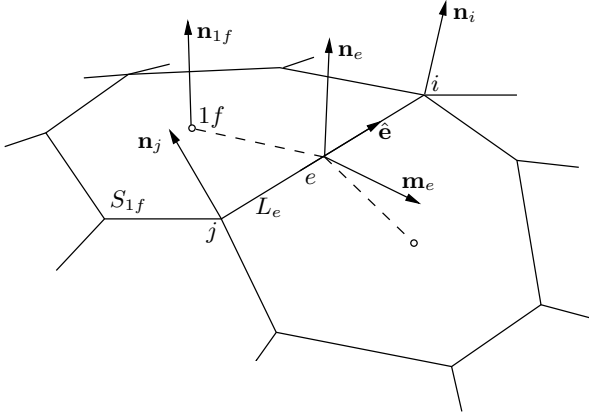


**Figure 7:** Control area  $S_{1f}$  at the interface.

It remains to decompose the surface tension force  $\mathbf{F}_{1f}^\sigma$  into the tangential component  $(\nabla_s \sigma)_{1f}$  used in Eq. (28), and the normal component  $(\kappa\sigma)_{1f} \mathbf{n}_{1f}$  used in Eq. (27). Using the surface Gauss integral theorem, surface tension force acting on the control area  $S_{1f}$  can be expressed by the following equation:

$$\mathbf{F}_{1f}^\sigma = \int_{S_{1f}} \nabla_s \sigma \, dS + \int_{S_{1f}} \kappa \sigma \mathbf{n} \, dS. \quad (42)$$

When the right hand side of Eq. (42) is discretised using the mid point rule and the result of the discretisation is equalised with the right hand side of Eq. (41), the following expression is obtained:

$$(\nabla_s \sigma)_{1f} + (\kappa\sigma)_{1f} \mathbf{n}_{1f} = \frac{1}{S_{1f}} \sum_e \sigma_e \mathbf{m}_e L_e. \quad (43)$$

Hence, the tangential component of the surface tension force acting on the control area  $S_{1f}$  is equal to the tangential component of the right hand side of Eq. (43):

$$(\nabla_s \sigma)_{Af} = \frac{1}{S_{Af}} (\mathbf{I} - \mathbf{n}_{Af} \mathbf{n}_{Af}) \cdot \sum_e \sigma_e \mathbf{m}_e L_e, \quad (44)$$

and its normal component is equal to the respective normal component:

$$(\kappa\sigma)_{Af} \mathbf{n}_{Af} = \frac{1}{S_{Af}} (\mathbf{n}_{Af} \mathbf{n}_{Af}) \cdot \sum_e \sigma_e \mathbf{m}_e L_e. \quad (45)$$

If the surface tension coefficient is constant ( $\sigma = \text{const.}$ ), Eq. (44) will give zero tangential component of the surface tension force if the normal unit vector of the control area  $S_{1f}$  satisfies the following equation:

$$\kappa_{1f} \mathbf{n}_{1f} = \frac{1}{S_{1f}} \sum_e \mathbf{m}_e L_e, \quad (46)$$

or, if  $\kappa_{1f} \neq 0$ :

$$\mathbf{n}_{1f} = \frac{\sum_e \mathbf{m}_e L_e}{|\sum_e \mathbf{m}_e L_e|}. \quad (47)$$

With Eqs. (44, 45 and 46) we shall formulate a procedure for calculation of surface tension force which ensures that total surface tension force on a closed surface will be exactly zero. Unfortunately, fulfilment of this condition is not sufficient for successful application of surface tension forces in the calculation. Specifically, unphysical fluid flow near the interface arise due to local (rather than global) inaccuracy in the calculation of surface tension forces.

From Eq. (41) one can see that the accuracy of surface tension force calculation depends on the accuracy of calculation of bi-normal unit vector  $\mathbf{m}_e$  which is calculated using the following expression:

$$\mathbf{m}_e = \hat{\mathbf{e}} \times \frac{\mathbf{n}_i + \mathbf{n}_j}{2}, \quad (48)$$

where  $\hat{\mathbf{e}}$  is the unit vector parallel with edge  $e$ , and  $\mathbf{n}_i$  and  $\mathbf{n}_j$  are the interface normal unit vectors in points  $i$  and  $j$  (see Fig. 7). Using Eq. (46) and (48) one obtains the exact value of curvature of the control area  $S_{1f}$  if points of the control area lie on the surface of the sphere.

### Solution procedure

Based on the described interface tracking method, one can now define the solution procedure for the Navier-Stokes system on a moving mesh, which may be used for simulation of two-phase fluid flow with the interface. The procedure consists of the following steps:

1. For the new time instance  $t = t^n$ , initialise the values of all dependent variables with the corresponding values from the previous time instance;
2. Define the displacement directions for the interface mesh points and the control points;
3. Start of outer iteration loop:
  - (a) Update pressure and velocity boundary conditions at the interface;
  - (b) Assemble and solve the discretised momentum equation (12) on the mesh with the current shape of the interface. The pressure field, face mass fluxes and volume fluxes are used from the previous (outer) iteration;

- (c) The velocity field obtained in the previous step is used for the assembly of discretised pressure equation (16). After the pressure equation is solved, the new absolute mass fluxes through the cell faces are calculated. Net mass flux through the interface is generally different from zero;
- (d) In order to compensate the net mass flux obtained in the previous step, the interface displacement is calculated using the interface points displacement procedure define in previous section;
- (e) The interface points displacement is used as a boundary condition for the solution of the mesh motion problem. After mesh displacement, the new face volume fluxes are calculated using the current points positions and the position from the previous time instance;
- (f) Convergence is checked and if the residual levels and the net mass flux through the interface do not satisfy the prescribed accuracy, the procedure is returned on step (a).

4. If the final time instance is not reached, return to step 1.

The efficiency of the above described solution procedure can be substantially increased if only the interface mesh points are moved in step (e) instead of moving all mesh points. In that case, the entire mesh is moved before the start of outer iteration loop, according to the total interface displacement obtained in the previous time step. Thus, the mesh motion procedure is performed only once in each time step, and overall procedure is more stable because the volume fluxes of the cell faces which are not in contact with the interface remains constant during the SIMPLE procedure. This approach is possible in the case when the magnitude of the interface mesh points displacement is less than the thickness of the cells near the interface. This condition is usually satisfied when time accuracy of the results is required.

### Conservation of volume

Volume conservation condition of the considered incompressible fluid phases depends on the satisfaction of kinematic condition at the interface. For the interface tracking procedure used in this study, volume conservation depends on the condition of zero net mass flux through the interface. Net mass flux through the interface can be reduced to an arbitrary level if a sufficient number of outer iterations is performed.

When the incompressible fluid phase 2 (see Fig. 4) is bounded by a closed boundary (without inlets or outlets), gradual reduction of the interface net mass flux during iterations can cause problems with the solution of the pressure equation. Specifically, on the 2 side of the interface belonging to phase 2, the normal derivative of modified pressure is zero and the velocity and mass flux are specified to ensure zero net mass flux through the

side 2 of the interface, *i.e.*

$$\dot{m}_{2f} = \rho_2 \dot{V}_{2f}. \quad (49)$$

Here,  $\dot{V}_{2f}$  is volume flux of the face  $2f$  at the 2 side of the interface. Since fluid 2 is incompressible, in order to solve the pressure equation, the total mass flux through the 2 side of the interface  $\sum_{2f} \dot{m}_{2f}$  must be identically zero. While this total mass flux will converge to zero during outer interactions, it will never be exactly zero. Therefore, the corrected mass flux through the side 2 of the interface is used in the pressure equation (16) as follows:

$$\dot{m}_{2f}^c = \dot{m}_{2f}^p - w_{2f} \sum_{2f} \dot{m}_{2f}^p, \quad (50)$$

where  $\dot{m}_{2f}^p$  is the mass flux through the face  $2f$  obtained in the previous outer iteration and  $w_{2f}$  is the weighting factor defined to ensure the mass flux correction distribution proportional to the mass fluxes distribution at side 2,

$$w_{2f} = \frac{|\dot{m}_{2f}^p|}{\sum_{2f} |\dot{m}_{2f}^p|}. \quad (51)$$

As the outer iterations advance, mass flux correction converges to zero and it does not influence the solution.

### NUMERICAL MODELLING OF A FREE-RISING BUBBLE

The method for numerical modelling of two-phase fluid flow with a sharp interface is defined with the final goal to simulate free-rising air bubbles in water, in the range of bubble diameter 1.3 – 6 mm. This is the flow regime where surface forces have dominant influence as described by Tomiyama et al. (2002). The bubble motion along a zig-zag and/or a helicoidal path is accompanied by a change of bubble shape.

Described interface tracking method is limited to problems where moderate change of interface shape occurs and there is no need to change mesh topology. This implies that the bubble must stay approximately in the centre of the spatial domain during the simulation. To accomplish this, approach proposed by Rusche (2002) is used, where the calculation is performed in a moving non-inertial coordinate system whose origin is attached to the centre of the bubble.

The spatial domain consisting of the bubble volume and the volume of surrounding liquid is shown on Fig. 4. The origin of the non-inertial coordinate system  $o'$  is placed in the centre of the bubble volume. Its position with respect to the origin  $o$  of the inertial coordinate system is determined by the vector  $\mathbf{r}_F$ . The switch away from a fixed to a moving coordinate system requires a correction of the momentum equation and its boundary conditions. One has to add the acceleration of the non-inertial coordinate system  $\mathbf{a}_F$  on the left hand side of momentum equation (2), where now  $\mathbf{v}$  is the fluid velocity in respect to the non-inertial coordinate system. If a bubble is rising through a still liquid, the value of fluid velocity specified on the outer boundary of the spatial domain is equal to the negative value of the moving

coordinate system velocity,  $\mathbf{v}_b = -\mathbf{v}_F$ . The velocity is specified only on the part of the outer boundary through which the fluid enters the domain; on the outlet part of the boundary the zero normal derivative is specified for pressure and velocity.

In the case when the effect of surfactants is considered, the surface transport equation for surfactant concentration (9) is solved at the beginning of each outer iteration. Newly obtained surfactant concentration field is used for calculation of new surface tension field by applying the surface equation of state (7).

Numerical simulation is performed for a rising air bubble in still water. The properties of water and air are taken at 20 °C. Radius of undeformed bubble is  $r_b = 1$  mm. Radius of the outer boundary is twenty times greater than the bubble radius, what is result of compromise between mesh size and influence of the outer boundary position on the solution. The initial bubble shape is spherical. Interface mesh points are moved in the direction of the interface normal from the previous time step.

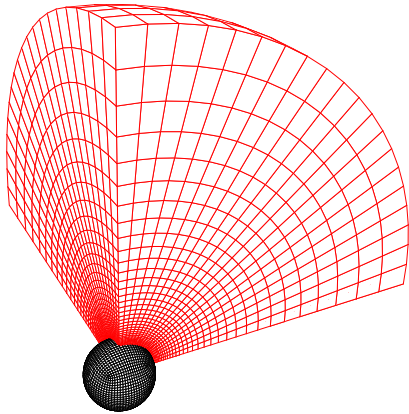


**Figure 8:** Section of a computational mesh for free-rising bubble simulations.

A part of the computational mesh is shown in Fig. 8. Mesh resolution is chosen according to the mesh sensitivity study performed by Blanco and Magnaudet (1995) for numerical modelling of axisymmetric bubbles of fixed shape in the range of Reynolds number  $\Re < 1000$ . The size of cells near the interface is  $0.01 r_b$  in the normal direction and  $0.04 r_b$  along the interface. The mesh consist 600 000 hexahedral cells, and the surface mesh on the interface consists 9000 quadrilateral finite areas.

#### Free-rising air bubble in clean water

We shall first consider a case with chemically clean water. The path lines behind the bubble are shown in Fig. 9. One can notice the existence of a double-threaded wake which is symmetric across the  $y-z$  plane crossing the bubble centre. This phenomenon is demonstrated by the visualisation of bubble wake performed by de Vries (2001).

Components of bubble centre velocity as a function of time are shown in Fig. 11. One can see that steady state

motion of the bubble is reached. The average rising velocity of the bubble is  $v_z = 0.325$  m/s. de Vries (2001) [also de Vries et al. (2002)] performed the experiment with the air bubble of radius  $r_b = 1$  mm in purified water. In the typical experiment the measured average rising velocity is  $v_z = 0.316$  m/s. The bubble moves along a zig-zag trajectory in the plane which approximately coincides with the  $x-z$  coordinate plane. This is in agreement with the experimental results obtained by de Vries (2001).

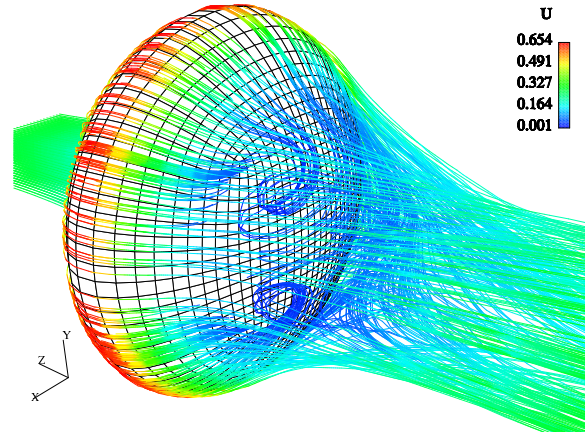


**Figure 9:** Path lines behind the rising 3-D air bubble in still water for clean bubble surface.

#### Free-rising air bubble in contaminated water

Finally air bubble rising through the water contaminated by surfactant is considered. At the beginning of calculation, volumetric concentration of the surfactant in water is uniform and amounts  $C = 0.01$  mol/m<sup>3</sup>, while the interface is clean ( $\Phi = 0$  mol/m<sup>2</sup>). Surfactant has the following properties: saturated concentration  $\Phi_\infty = 5 \times 10^{-6}$  mol/m<sup>2</sup>, surface diffusivity  $D_s = 5 \times 10^{-6}$  m<sup>2</sup>/s, bulk diffusivity  $D = 5 \times 10^{-6}$  m<sup>2</sup>/s, adsorption coefficient  $k_a = 400$  m<sup>3</sup>/(mols) and desorption coefficient  $\beta = 0.3$  mol/m<sup>3</sup>.

Fig. 10 shows the velocity field and bulk and surface surfactant concentration in the  $x-z$  plane crossing the bubble centre.

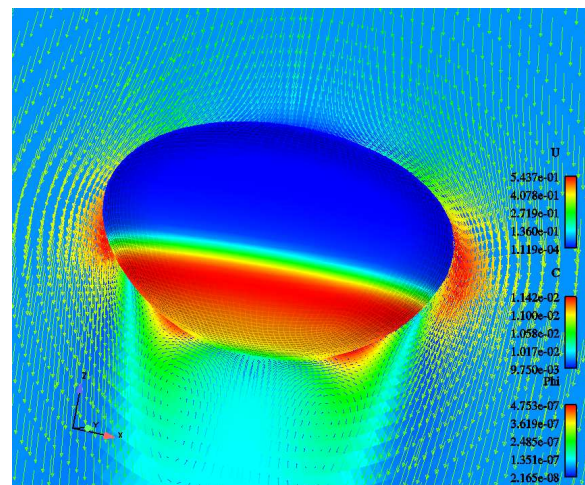


**Figure 10:** Flow field and surfactant concentration for bubble with contaminated interface.

Components of bubble centre velocity as a function of time are shown in in Fig. 12. The bubble moves along a helicoidal trajectory. The rising velocity is approximately constant with time and amounts to  $v_z = 0.25$  m/s, 15 %

less than the average rising velocity with a clean surface.

Deformation of contaminated bubble is substantially lower than deformation of the clean bubble. The ratio between major and minor semi-axis of the bubble is 1.38 for the contaminated bubble, and 1.95 for the clean bubble.

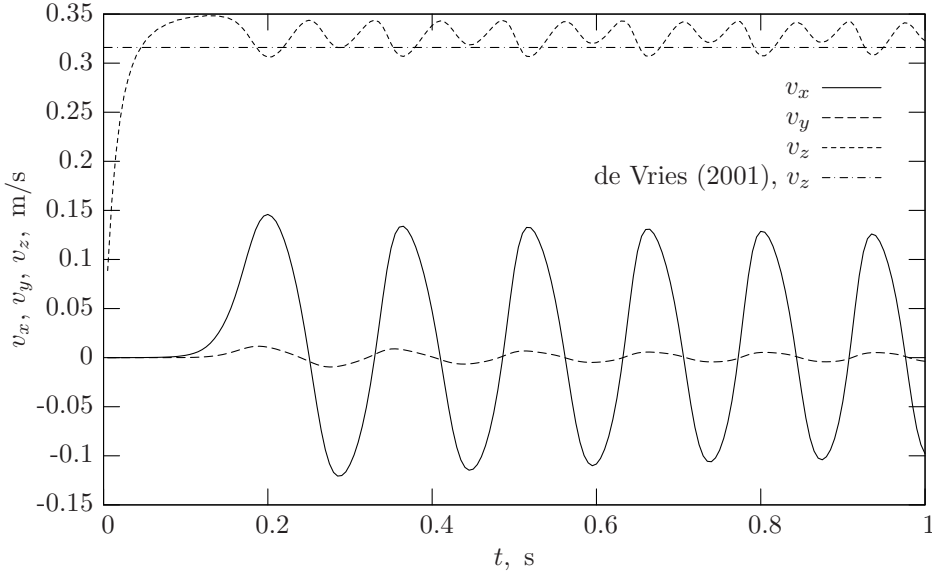


**Figure 11:** Velocity of the bubble centre as a function of time for clean bubble.

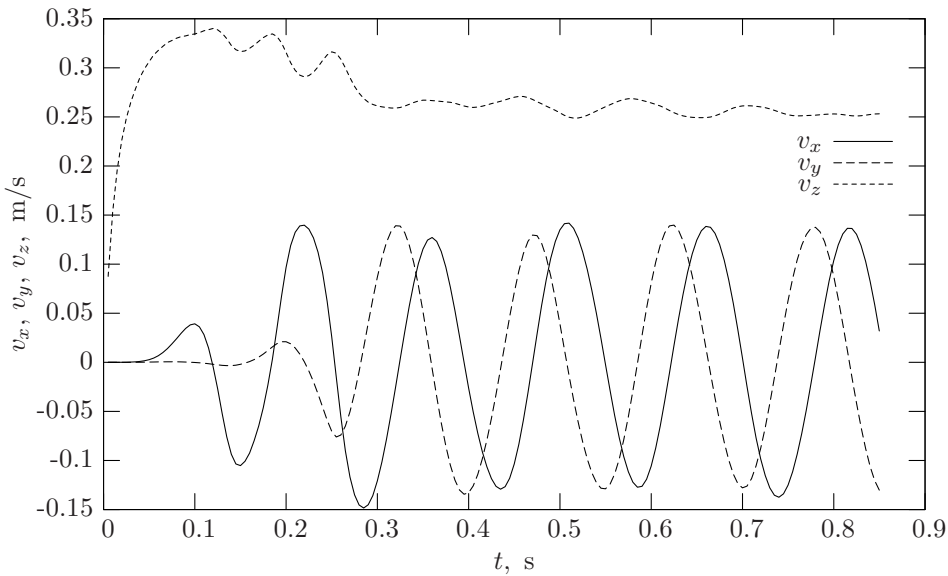


**Figure 12:** Velocity of the bubble centre as a function of time for contaminated bubble.

## CONCLUSION

Interface tracking method is developed for simulation of two-fluid system with a sharp interface and soluble surfactants. Finite volume method is used for discretisation of volumetric transport equations on a moving computa-

tional mesh and finite area method is used for discretisation of surface transport equation on curved moving surface mesh. Method is applied for calculation of free-rising air bubble in clean and contaminated water. Result show good agreement with available experimental results.

## REFERENCES

- F. R. Batchelor. *An introduction to fluid dynamics*. Cambridge University Press, Cambridge, 1967.
- A. Blanco and J. Magnaudet. The structure of the axisymmetric high-Reynolds number flow around an ellipsoidal bubble of fixed shape. *Physics of fluids*, 7(6):1265–1274, 1995.
- A. W. G. de Vries. *Path and wake of a rising bubble*. PhD thesis, University of Twente, 2001.
- A. W. G. de Vries, A. Biesheuvel, and L. van Wijngaarden. Notes on the path and wake of a gas bubbles rising in pure water. *International journal of multiphase flow*, 28:1823–1835, 2002.
- I. Demirdžić and S. Muzaferija. Numerical method for coupled fluid flow, heat transfer and stress analysis using unstructured moving meshes with cells of arbitrary topology. *Computer methods in applied mechanics and engineering*, 125:235–255, 1995.
- I. Demirdžić and M. Perić. Space conservation law in finite volume calculations of fluid flow. *International journal for numerical methods in fluids*, 8: 1037–1050, 1988.
- M. A. Drumright-Clarke and Y. Renardy. The effect of insoluble surfactant at dilute concentration on drop breakup under shear with inertia. *Physics of fluids*, 16(1):14–21, 2004.
- D. A. Edwards, H. Brenner, and D. T. Wasan. *Interfacial transport processes and rheology*. Butterworth-Heinemann, 1991.
- J. H. Ferziger and M. Perić. *Computational methods for fluid dynamics*. Springer Verlag, Berlin-New York, 1995.
- A. J. James and J. Lowengrub. A surfactant-conserving volume-of-fluid method for interfacial flows with insoluble surfactants. *Journal of computational physics*, 201(2):685–722, 2004.
- H. Jasak. *Error analysis and estimation for finite volume method with applications to fluid flows*. PhD thesis, Imperial College, University of London, 1996.
- H. Jasak and Ž. Tuković. Automatic mesh motion for the unstructured finite volume method. *Transaction of FAMENA*, 30(2):1–20, 2006.
- H. Jasak and H. G. Weller. Application of the finite volume method and unstructured meshes to linear elasticity. *International journal for numerical methods in engineering*, 48:267–287, 2000.
- H. Jasak, H. G. Weller, and A. D. Gosman. High resolution NVD differencing scheme for arbitrarily unstructured meshes. *International journal for numerical methods in fluids*, 31:431–449, 1999.
- J. Lee and C. Pozrikidis. Effect of surfactants on the deformation of drops and bubbles in navier-stokes flow. *Computers and fluids*, 35:43–60, 2006.
- M. Muradoglu and G. Tryggvason. A front tracking method for computation of interfacial flows with soluble surfactants. *Journal of computational physics*, 227(4):2238–2262, 2008.
- S. Muzaferija and M. Perić. Computation of free-surface flows using the finite-volume method and moving grids. *Numerical heat transfer, Part B*, 32: 369–384, 1997.
- H. Rusche. *Computational fluid dynamics of dispersed two-phase flows at high phase fractions*. PhD thesis, Imperial College, University of London, 2002.
- A. Tomiyama, G. P. Celata, S. Hosokawa, and S. Yoshida. Terminal velocity of single bubbles in surface tension force dominant regime. *International journal of multiphase flow*, 28:1497–1519, 2002.
- Ž. Tuković. *Finite volume method on domains of varying shape (in Croatian)*. PhD thesis, Faculty of Mechanical Engineering and Naval Architecture, University of Zagreb, 2005.
- C. E. Weatherburn. *Differential geometry in three dimension*. Cambridge University Press, London, 1972.
- J.-J. Xu, Z. Li, J. Lowengrub, and H. Zhao. A level-set method for interfacial flows with surfactant. *Journal of computational physics*, 212(2):590–616, 2006.
- J. Zhang, D. M. Eckmann, and P. S. Ayyaswamy. A front tracking method for a deformable intravascular bubble in a tube with soluble surfactant transport. *Journal of computational physics*, 214(1):366–396, 2006.